http://journal.uir.ac.id/index.php/saintis

Jurnal Saintis

ISSN (Print) : 1410-7783
ISSN (Online) : 2580-7110

Volume 26 Nomor 02, Oktober 2026 : 119-136

Effect of Shear Wall Configuration on Torsional Response and Seismic Performance of Irregular Buildings

Ayu Sinta Aprilia[1,*], Andi S.[1], Rahmat Kurniawan[1], Kirtinanda P.[1], Siska Apriwelni[1], Ahmad Auliadi Yufrizal[1]

[1] *Civil Engineering Study Program, Faculty of Infrastructure and Regional Planning, Institut Teknologi Sumatera, South Lampung, Lampung 35365, Indonesia*

* Corresponding author: ayu.aprilia@si.itera.ac.id
Tel.: +62-856-4513-4326
Received: Sep 25, 2026; Revision: Oct 29, 2026; Accepted: Oct 31, 2026
DOI: 10.25299/saintis.2026.vol26(02).30339

Abstract

Indonesia lies in a region of high seismic intensity, so earthquake-resistant design is essential for buildings in high-risk categories. This study evaluates the seismic performance of the Public Service Building (GLU) of Institut Teknologi Sumatera (ITERA), a seven-story reinforced concrete building with an irregular plan, classified as Risk Category IV, under five shear wall placement configurations: SWC-Full, CW-Only, SW-Only, SWC-Dist and SW-Multi. The structure was modeled in ETABS as a dual system and analyzed using response spectrum analysis in accordance with SNI 1726:2019 and nonlinear static pushover analysis based on FEMA 440. Seven parameters were assessed: structural period and modal response, inter-story drift, P-Delta stability, dual system effectiveness, element compliance with the Special Moment-Resisting Frame (SMRF) requirements of SNI 2847:2019, shear wall capacity, and pushover performance level. The results show that the centralized configuration (SWC-Full) produces a dominant torsional first mode (RZ), whereas the distributed configuration (SWC-Dist) produces a translational first mode (UX). The X-direction period ranges from 0.876 s (SWC-Dist) to 1.673 s (SW-Only). Only SWC-Full and SWC-Dist satisfy all seven evaluation criteria simultaneously, with drift-based performance levels between Immediate Occupancy (IO) and Life Safety (LS) and practically equivalent relative scores (0.92 and 0.90). Removing the core wall (SW-Only) causes drift and beam failures, including a 42% exceedance of beam flexural strength, and leaves the walls only 13% of the X-direction base shear. These findings indicate that, for irregular Risk Category IV buildings, the shear wall–core wall combination is the decisive factor in satisfying the seismic requirements.

Keywords: shear wall configuration, irregular building, dual system, pushover analysis, FEMA 440

INTRODUCTION

Indonesia is located at the convergence of three major tectonic plates, namely the Indo-Australian, Eurasian and Pacific plates, making it one of the most seismically active regions in the world. The Sumatran subduction zone, stretching from Aceh to Lampung, is one of the most active earthquake sources, with a peak ground acceleration (PGA) of 0.465g at a 7% probability of exceedance in 75 years in the Sunda Strait area [1]. This seismotectonic condition demands earthquake-resistant structural design, particularly in Lampung Province, which is experiencing rapid growth in educational infrastructure.

The Public Service Building (Gedung Layanan Umum, GLU) of Institut Teknologi Sumatera (ITERA) is a seven-story educational facility serving thousands of students and is classified as a Risk Category IV building under SNI 1726:2019 [2]. The building is characterized by an irregular floor plan geometry, which is structurally more susceptible to torsional effects and non-uniform deformation than regular buildings [3]. Ruggieri and Vukobratović [4] further showed that torsion amplifies not only displacement but also floor acceleration demands in low-rise reinforced concrete buildings, so torsional behavior must be checked explicitly rather than inferred from global drift alone. The choice of the lateral force-resisting element configuration, particularly that of the shear walls, is therefore a critical aspect of the structural design.

Shear walls are highly effective structural elements for resisting lateral earthquake forces [5]. Shamrao [6] showed probabilistically that, in torsionally imbalanced buildings, shear walls markedly reduce the probability of damage and equalize the response in both orthogonal directions. In multi-story buildings with a dual system, shear walls work together with moment-resisting frames to resist seismic forces; the frames must be capable of carrying at least 25% of the design seismic force [2]. The effectiveness of the dual system is strongly influenced by the shear wall placement configuration, which determines the lateral stiffness

distribution, the torsional response and the overall deformation capacity of the structure [7].

Several prior studies have examined the effect of shear wall placement on structural performance. Katrangi et al. [8] assessed the seismic performance and base shear contribution ratios of reinforced concrete wall-frame dual systems and confirmed that dual system effectiveness depends on the proportional stiffness of each lateral force-resisting element. Dumalanta et al. [9] evaluated three shear wall configurations in a five-story irregular building and found that the outer-center (distributed) configuration provided the most balanced seismic response, improving the performance level from Life Safety (LS) to Immediate Occupancy (IO) based on FEMA 440. Khelaifia et al. [10] reported that symmetric and complete shear wall configurations produce the smallest drift values, while Barser et al. [11] demonstrated a positive correlation between the completeness of lateral elements and drift limit compliance. Kurnia et al. [12] compared three shear wall positions in an irregular building using response spectrum analysis and found that the most effective position reduced the maximum lateral displacement by about 40% relative to the building without shear walls. Aslani and Tehrani [3] examined the effect of vertical irregularities in shear walls on the collapse capacity of dual system structures and showed that the vertical position of the irregularity is a critical parameter that is not yet accommodated by current seismic design standards. Salmassi et al. [13] demonstrated that the position of end shear walls in tall buildings with torsional irregularity governs the distribution of wall stresses and the overall performance, while Yakhkeshi and Tehrani [14] analyzed seven dual frame–shear wall models and found that local wall inclination affects collapse resistance more strongly than global torsional irregularity, indicating that the geometric arrangement of the walls, and not only the total wall area, governs seismic performance.

Although shear wall placement has been studied widely, three gaps remain. First, most studies use regular or symmetric building models in the lower risk categories (II and III), whereas irregular Risk Category IV buildings, for which the code imposes the strictest drift limits and the redundancy factor, have received little attention. Second, the evaluations are usually limited to global indicators such as period, drift or base shear, so the link between the wall layout and the element-level SMRF compliance of the frames is not examined. Third, the dual system is normally checked only against the 25% minimum frame share, although the actual distribution of base shear between walls and frames can differ greatly between layouts. To the authors' knowledge, these aspects have not been evaluated together for an existing irregular Risk Category IV building in Indonesia.

Based on these gaps, the present study aims to (1) evaluate the effect of five shear wall configurations on the structural period, inter-story drift and torsional response; (2) analyze the dual system of each configuration, both against the code requirement and in terms of the actual force share; and (3) compare the pushover performance of the configurations in order to determine the most suitable shear wall placement for an irregular Risk Category IV building. The original contributions of this study are: (i) a side-by-side evaluation of five wall layouts of an existing irregular Risk Category IV building designed to SNI 1726:2019 and SNI 2847:2019; (ii) an integrated framework that links each layout to its torsional irregularity, dual system force share, SMRF element compliance and pushover performance within one consistent set of models; and (iii) evidence that a layout can satisfy the 25% dual system requirement while its walls carry only 13% of the base shear, which leads to beam failures that global drift checks do not reveal.

METHOD

Study Object Description

The case study building is the ITERA Public Service Building (GLU), located in South Lampung Regency, Lampung Province, at coordinates 5.36289° S and 105.31377° E (Figure 1). The building has seven stories and a total height of 32.5 m; the first two stories are 5 m high and the remaining five stories are 4.5 m high. The floor plan is irregular, with overall dimensions of 56 m × 50.77 m. The structural materials comprise concrete with a specified compressive strength (f'_c) of 30 MPa, longitudinal reinforcement with a yield strength (f_y) of 420 MPa (BjTS 420A) and transverse reinforcement with a yield strength (f_{yt}) of 280 MPa (BjTP 280). The principal member dimensions are beam B1 (350 × 650 mm), column K1 (700 × 700 mm), shear wall thickness 400 mm and slab thickness 130 mm. The plan comprises seven 8 m bays in the X direction and has a re-entrant corner (horizontal irregularity Type 2 of SNI 1726:2019 [2]) in all configurations.

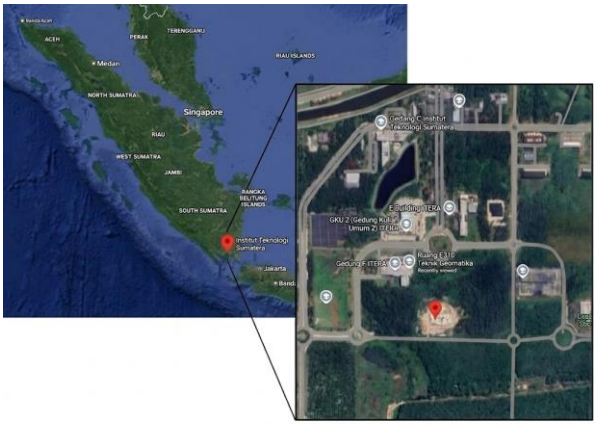


Figure 1. Location of the ITERA Public Service Building in South Lampung

Shear Wall Configurations

The five shear wall configurations evaluated in this study are shown in Figure 2. The naming convention is based on the type of lateral element and its distribution characteristics.

(1) SWC-Full (full central SW–CW): the existing configuration with complete shear wall (SW) and core wall (CW), centrally positioned in the building. It serves as the comparison baseline.

(2) CW-Only (central CW without SW): retains only the core wall without additional shear walls, which removes the lateral stiffness elements along the building perimeter.

(3) SW-Only (peripheral SW without CW): retains the shear walls along the building perimeter but omits the core wall, eliminating the central stiffness core of the building.

(4) SWC-Dist (distributed SW–CW): an alternative configuration with a core wall and varied shear wall positions distributed differently from SWC-Full.

(5) SW-Multi (multidirectional SW without CW): shear walls oriented in the X direction replace the core wall and act together with the original shear walls, forming linear multidirectional elements without a closed core.

Figure 2 shows the global X and Y axes and the layout of the lateral elements in each configuration. The core wall (CW) is a closed box between grid lines 4 and 5 above the central void, with its longer side along the X direction. The planar shear walls (SW) are 400 mm thick and 4.7 m long including their boundary columns, and they are oriented in the Y direction. In SWC-Full and SW-Only they are on grid lines 3 and 6; in SWC-Dist they are moved to the end bays, between grid lines 1 and 2 and between grid lines 7 and 8; and in SW-Multi the core is replaced by a planar wall along the X direction between grid lines 4 and 5 (PSW3), which acts with the two Y-direction walls on grid lines 3 and 6 (PSW1 and PSW2). All other members are identical in the five models. The centers of mass and rigidity were not exported from the ETABS models; the plan eccentricity is therefore characterized through the torsional irregularity ratios of all configurations (Tables 2 and 3).

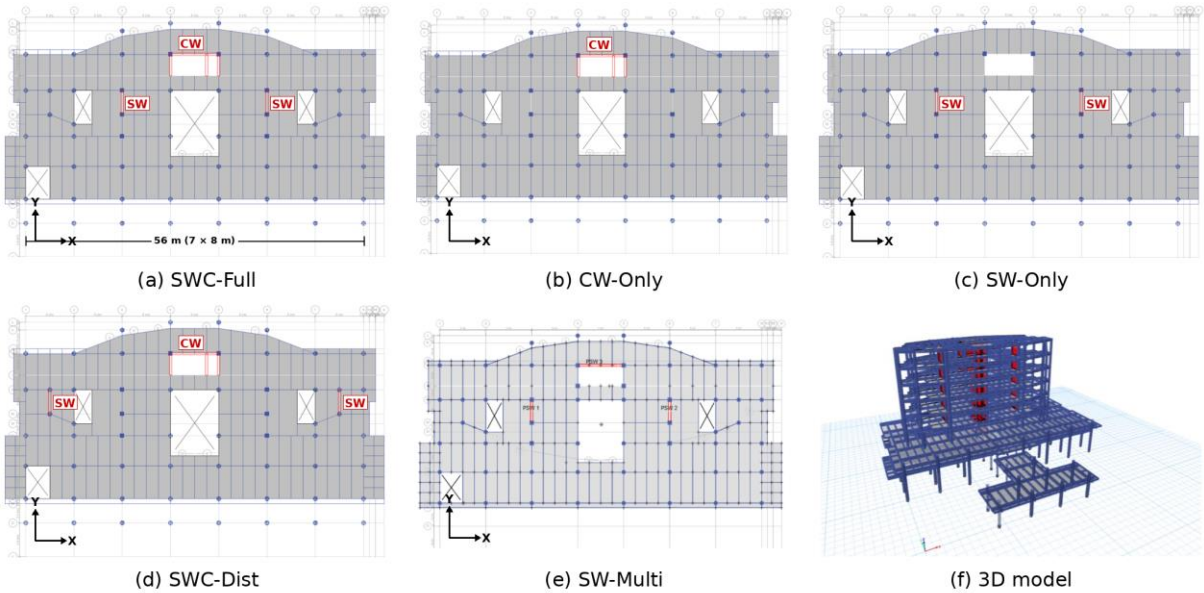


Figure 2. Typical Floor Plans and Three-Dimensional Model of the ITERA GLU (Red: Shear Walls and Core Wall; Grid Spacing 8 m in the X Direction; Overall Plan 56 m × 50.77 m)

Seismic Design Parameters

Seismic acceleration parameters were obtained from the RSA Cipta Karya web application based on SNI 1726:2019 for the building site, which is classified as site class SD, i.e., stiff soil [15]. The key design parameters are shown in Figure 3: the mapped spectral response acceleration at short periods (S_s) is 0.8291g and that at a period of 1 s (S_1) is 0.4138g. Using a short-period site coefficient (F_a) of 1.1684 and a 1 s site coefficient (F_v) of 1.8862, the design spectral response acceleration at short periods (S_{DS}) is 0.6458g and that at a period of 1 s (S_{D1}) is 0.5203g. Based on these values, the structure is assigned to Seismic Design Category (SDC) D. For Risk Category IV, the seismic importance factor (I_e) is 1.5, the response modification coefficient (R) is 7, the system overstrength factor (Ω_0) is 2.5 and the deflection amplification factor (C_d) is 5.5. The approximate fundamental period (T_a), computed from the empirical expression of SNI 1726:2019, is 0.6643 s, with an upper-bound period $T_{max} = C_u \cdot T_a$ = 0.930 s.

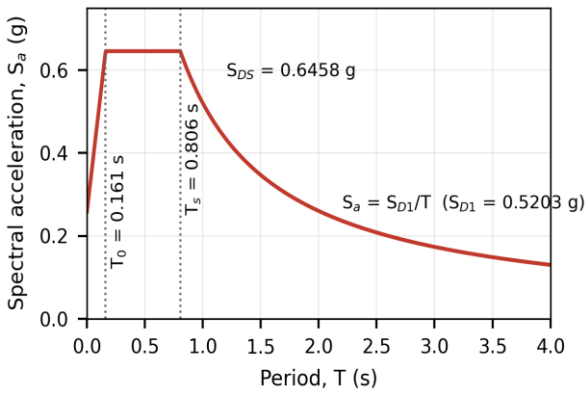


Figure 3. Design Response Spectrum for the ITERA GLU Site

Loading

The loads were determined in accordance with SNI 1727:2020 [16]. The superimposed dead load (SDL) comprises ceramic tiles, 0.24 kN/m^2; mechanical ducting, 0.25 kN/m^2; ceiling and frame, 0.14 kN/m^2; mortar screed, 0.61 kN/m^2; and autoclaved aerated concrete (AAC) block walls, 5.8 kN/m^2 and 6.6 kN/m^2. The live loads vary with occupancy: cafeteria and lobby, 4.79 kN/m^2; office, 2.4 kN/m^2; toilet, 1.92 kN/m^2; archive room, 3.6 kN/m^2; corridor, 3.83 kN/m^2; and roof, 0.96 kN/m^2. The wind load was based on a basic wind speed of 40 m/s and Exposure Category B. The load combinations followed SNI 1726:2019, and orthogonal seismic effects were accounted for using the 100%–30% directional combination rule.

Modeling and Analysis

The structure was modeled in ETABS v22.0.0 (Extended Three-dimensional Analysis of Building Systems) as a three-dimensional model with fixed supports at the base and a rigid diaphragm assigned at each floor level. Cracked-section stiffness modifiers were applied in accordance with SNI 2847:2019 to account for cracking of the reinforced concrete members, namely (Table 6.6.3.1.1(a)) 0.70I_g for columns and for shear walls (the uncracked-wall value) and 0.35I_g for beams, where I_g is the gross moment of inertia [17]. The linear analysis used the response spectrum method with base shear scaling [18]. The nonlinear analysis used a displacement-controlled static pushover procedure up to 4% of the total height (1,300 mm); the procedures and limitations of this technique have been reviewed comprehensively by Kuria and Kegyes-Brassai [19]. Plastic hinges were defined at beam ends (0.1L and 0.9L) using Auto M3 hinges (strong-axis flexure, ASCE 41-17 Table 10-7) and at column ends using Auto P-M2-M3 hinges (biaxial flexure–axial interaction, ASCE 41-17 Table 10-8) [20]; the IO, LS and CP acceptance criteria (plastic rotations) of the same tables were assigned to each hinge. The shear walls were modeled as elastic shell elements, as explained below.

The modal analysis used 25 modes. The cumulative modal mass participation ratios in UX, UY and RZ were 97.8%, 94.5% and 98.7% for SWC-Full; 97.5%, 95.2% and 99.0% for CW-Only; 99.9%, 95.3% and 98.2% for SW-Only; 98.3%, 95.4% and 96.4% for SWC-Dist; and 97.3%, 96.6% and 98.5% for SW-Multi. All exceed the 90% minimum of SNI 1726:2019 Pasal 7.9.1.1 [2] in both horizontal directions. The pushover analysis started from a nonlinear gravity case (1.0D + 1.0SIDL + 0.25L), was run under displacement control up to 1,300 mm, and monitored the roof displacement at the center of mass of the roof diaphragm.

The shear walls were modeled as elastic shell elements with the stiffness of 0.70I_g, whereas plastic hinges were assigned only to the beams and columns. In the SMRF–special wall dual system considered here, the frame hinges are the intended energy-dissipating mechanism, and the walls were verified separately by the force-based checks of SNI 2847:2019 [17]: axial–flexural interaction with SP-Column, minimum reinforcement, special boundary elements and shear capacity (Table 6). This approach keeps the five models comparable under identical assumptions, but flexural yielding, shear cracking and stiffness degradation of the walls are

not represented. The nonlinear response of the system is therefore governed by the frame hinges, and the capacity curves are stiffer and stronger than those of a model with nonlinear walls; the base shear capacity in particular is overestimated. The target displacements and performance levels should consequently be read as comparative indicators between the configurations rather than as absolute estimates of the nonlinear capacity. This limitation is most relevant for CW-Only, whose core wall fails the shear capacity check (Table 6), so its pushover response is unconservative.

The target displacement was computed using the coefficient (displacement modification) method of FEMA 356 Section 3.3.3.3.2 [21], which FEMA 440 [22] reviewed and retained in the same form, expressed in Equation (1). The spectral acceleration and effective period at the performance point were obtained from the FEMA 440 equivalent linearization procedure in ETABS, as also adopted by Sugianto and Pranata [23], and the target displacement was then evaluated with the coefficient expression, following the procedure applied by Usman et al. [24] to reinforced concrete shear wall buildings in several Indonesian seismic regions, so that its output maps directly onto the drift-based performance limits used in this study.

$$\delta_T = C_0 C_1 C_2 C_3 \cdot S_a \cdot (T_e^2/4\pi^2) \cdot g \qquad (1)$$

where C_0 is the modification factor relating the spectral displacement to the roof displacement (1.2, taken from FEMA 356 Table 3-2), C_1 is the modification factor relating the maximum inelastic displacement to the elastic displacement, C_2 is the modification factor accounting for pinched hysteresis, stiffness degradation and strength deterioration, C_3 is the P-Delta factor, S_a is the spectral acceleration at the performance point and T_e is the effective period, both obtained from the FEMA 440 equivalent linearization output of ETABS, and g is the acceleration of gravity (9.81 m/s^2). In accordance with FEMA 356 Section 3.3.3.3.2, $C_1 = 1.0$ was adopted because the effective period of every configuration exceeds the characteristic period of the design response spectrum, $T_s = S_{D1}/S_{DS} = 0.806$ s ($T_e \geq T_s$), $C_2 = 1.0$, which the same section permits for nonlinear procedures, and $C_3 = 1.0$ because the capacity curves have a positive post-yield stiffness.

Evaluation Parameters

Structural performance was evaluated against seven parameters: (1) the inter-story drift limit of SNI 1726:2019, set at 0.77% of the story height for Risk Category IV with a redundancy factor of 1.3; (2) the P-Delta stability coefficient ($\theta < \theta_{allow} = 0.0909$); (3) the dual system requirement of SNI 1726:2019 Pasal 7.2.5.1 [2], under which the moment frame must resist at least 25% of the design seismic force, together with the effectiveness of the force share between frame and walls; (4) beam compliance with the SMRF requirements of SNI 2847:2019, covering flexural strength ($\phi M_n > M_u$), shear strength ($\phi V_n/V_u \geq 1$) and torsional demand; (5) column compliance with the strong column–weak beam (SCWB) criterion; (6) shear wall adequacy, covering minimum reinforcement, special boundary element confinement ($A_{sh}/s \geq (A_{sh}/s)_{min}$) and shear capacity; and (7) the pushover performance, obtained from the FEMA 440 target displacement as described below. The SCWB criterion is expressed in Equation (2).

$$\Sigma M_{nc} \geq 1.2\, \Sigma M_{nb} \qquad (2)$$

where ΣM_{nc} is the sum of the nominal flexural strengths of the columns above and below the joint ($\Sigma M_{nc} = 2M_{nc}$ for identical columns) and $\Sigma M_{nb} = M_n^- + M_n^+$ is the sum of the nominal flexural strengths of the beams framing into the joint.

Three quantities are distinguished in the pushover evaluation and are not treated as identical. The performance point is the intersection of the capacity spectrum with the FEMA 440 modified demand spectrum (equivalent linearization) and gives S_a, S_d and T_e [22]. The target displacement δ_T is the roof displacement demand obtained from Equation (1) with S_a and T_e at the performance point. The component acceptance criteria are the IO, LS and CP plastic rotation limits of ASCE 41-17 [20] assigned to the beam and column hinges; they are checked at the analysis step closest to δ_T.

The global performance level is obtained by converting δ_T into the roof drift ratio δ_T/H, where H = 32.5 m is the height of the monitored roof node above the fixed base, and comparing it with the drift values given for concrete frames in FEMA 356 Table C1-3 [21]: 1% transient drift for IO, 2% for LS and 4% for CP, that is 325 mm, 650 mm and 1,300 mm. FEMA 440 does not define these thresholds itself; it improves the nonlinear static procedures of FEMA 356 and ATC-40 that are used here to compute the demand. FEMA 356 states that these drift values are typical values that illustrate the overall response and are not acceptance criteria. The drift-based level is therefore used only as a common global indicator for comparing the configurations, and it is reported

together with the hinge states at δ_T (Table 12). The concrete-frame values were adopted because the inelastic response of the model is concentrated in the frame hinges. The same table gives stricter values for concrete walls (0.5%, 1% and 2%); applying them would lower the global level of every configuration by one category, so the drift-based levels reported here are upper-bound estimates.

RESULTS AND DISCUSSION

Structural Period and Modal Response

Table 1 summarizes the structural periods of the five configurations. The fundamental period T_1 varies significantly: SW-Only has the highest value (1.673 s), indicating the most flexible structure due to the removal of the core wall, whereas SWC-Dist has the lowest value (0.876 s). SWC-Dist is the only configuration whose fundamental period is shorter than the upper-bound period T_{max} = 0.930 s, so it is also the only configuration for which the computed rather than the code-limited period governs the design in the X direction.

Table 1. Summary of Structural Periods and Mode Shapes

Parameter	SWC-Full	CW-Only	SW-Only	SWC-Dist	SW-Multi	Unit
T_1 (mode 1)	1.014	1.223	1.673	0.876	1.025	s
T_2 (mode 2)	0.778	0.904	0.985	0.824	0.980	s
T_{UY} (first UY mode)	0.778	0.904	0.968	0.824	0.980	s
T_X (design)	0.930	0.930	0.930	0.876	0.930	s
T_Y (design)	0.778	0.904	0.930	0.824	0.930	s
Mode 1	RZ	RZ	UX	UX	UX	–
Mode 2	UY	UY	RZ	UY	UY	–
Mode 3	UX	UX	UY	UX	UX	–

Note: T_1 and T_2 are the periods of the first and second ETABS modes. T_{UY} is the period of the lowest mode with dominant translational mass participation in the Y direction, which for SW-Only is the third mode (0.968 s) because its second mode is torsional. T_X and T_Y are the periods adopted for design, limited by $T_{max} = C_u \cdot T_a$ = 0.930 s.

A key finding of the modal analysis (Figure 4) is the difference in torsional response among the configurations. SWC-Full and CW-Only exhibit a first mode of rotation about the vertical axis (RZ) with torsional mass participation ratios of 0.242 and 0.266, respectively, indicating a dominant torsional response caused by the centralized shear wall position. In contrast, SW-Only, SWC-Dist and SW-Multi exhibit a first mode of translation in the X direction (UX), because the dispersed lateral elements increase the torsional stiffness. This result is consistent with Dumalanta et al. [9], who showed that the outer-center (distributed) configuration produces a more balanced seismic response than the centralized configuration, and with Aslani and Tehrani [3], who emphasized the influence of the spatial distribution of the lateral elements on the torsional response of dual system structures.

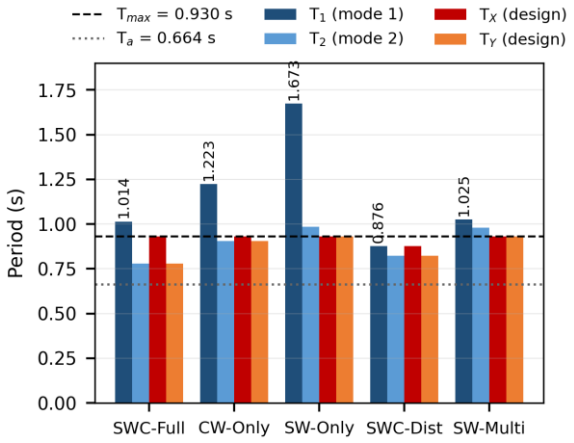


Figure 4. Comparison of Structural Periods Among Shear Wall Configurations

Table 2 presents the torsional irregularity check for the SWC-Full configuration. The ratio of maximum to average displacement ($\Delta_{max}/\Delta_{avg}$) was evaluated at each floor level in both principal directions. Following SNI 1726:2019 Table 13, a ratio exceeding 1.2 is classified as torsional irregularity (H.1a) and a ratio exceeding 1.4 as extreme torsional irregularity (H.1b).

Table 2. Torsional Irregularity Ratio ($\Delta_{max}/\Delta_{avg}$) of the SWC-Full Configuration

Floor	$\Delta_{max}/\Delta_{avg}$ (X)	Status X	$\Delta_{max}/\Delta_{avg}$ (Y)	Status Y
8	1.312	H.1a	1.146	OK
7	1.327	H.1a	1.155	OK
6	1.341	H.1a	1.163	OK
5	1.347	H.1a	1.169	OK
4	1.336	H.1a	1.167	OK
Elv 10.4	1.428	H.1b	1.364	H.1a
3	1.319	H.1a	1.597	H.1b
Elv 9	1.417	H.1b	1.157	OK
Elv 6.53	1.400	H.1b	1.399	H.1a
Elv 5.13	1.488	H.1b	1.167	OK
2	1.405	H.1b	1.201	H.1a

All five configurations exhibit H.1a or H.1b irregularity in at least one direction (Table 3). Consequently, the accidental torsional moment was amplified using the torsional amplification factor A_x given by Equation (3).

$$A_x = (\Delta_{max} / 1.2\,\Delta_{avg})^2 \le 3.0 \qquad (3)$$

For SWC-Full, the largest amplification factors were A_x = 1.538 in the X direction (elevation 5.13 m) and A_x = 1.771 in the Y direction (story 3), corresponding to accidental eccentricities of 3.903 m (7.7% of the building dimension) and 4.959 m

(8.9%), respectively. A redundancy factor ρ = 1.3 was also applied to the drift limits, as required for structures exhibiting extreme torsional irregularity (H.1b).

Table 3 extends the check to all configurations. Extreme torsional irregularity (H.1b) occurs in both directions in SWC-Full, CW-Only, SW-Only and SWC-Dist, and in the Y direction of SW-Multi, whose X direction remains H.1a (maximum 1.280). The largest ratio is 1.681 (SWC-Dist, Y direction, story 3), so distributing the walls changes the mode sequence but does not remove the irregularity class. In all configurations the maxima occur at stories 2 and 3 and at the partial intermediate levels between elevations 5.13 m and 10.4 m, where the absolute drifts are small. At stories 4 to 8 the X-direction ratios are 1.06–1.11 for SW-Only and 1.09–1.12 for SW-Multi, whose walls are not concentrated at the core, compared with 1.31–1.35 for SWC-Full and SWC-Dist and 1.22–1.42 for CW-Only. The amplification factor A_x was computed for every configuration and applied to the accidental eccentricity.

Table 3. Maximum Torsional Irregularity Ratio ($\Delta_{max}/\Delta_{avg}$) of All Configurations

Configuration	Max. ratio X (level)	Max. ratio Y (level)	Type X / Y	$A_{x,max}$
SWC-Full	1.488 (Elv 5.13)	1.597 (3)	H.1b / H.1b	1.771
CW-Only	1.516 (Elv 5.13)	1.631 (3)	H.1b / H.1b	1.847
SW-Only	1.590 (Elv 6.53)	1.577 (3)	H.1b / H.1b	1.756
SWC-Dist	1.454 (Elv 5.13)	1.681 (3)	H.1b / H.1b	1.962
SW-Multi	1.280 (2)	1.584 (3)	H.1a / H.1b	1.742

Note: level of the maximum in parentheses (story number or partial level elevation in m); $A_{x,max} = (\Delta_{max}/1.2\Delta_{avg})^2$ for the larger ratio of the two directions.

Inter-Story Drift and P-Delta Stability

The inter-story drift limit for Risk Category IV is 0.77% of the story height (1% divided by the redundancy factor of 1.3). The analysis shows that only SWC-Full and SWC-Dist satisfy the drift limit in both directions. CW-Only fails in the Y direction, while SW-Only and SW-Multi fail in both directions, as shown in Figure 5 and Figure 6. The commonality between the two compliant configurations is that both retain the complete combination of shear wall and core wall; removing either element causes the drift to exceed the allowable limit. This finding is consistent with Khelaifia et al. [10] and Barser et al. [11], who reported a positive correlation between the completeness of lateral elements and drift limit compliance.

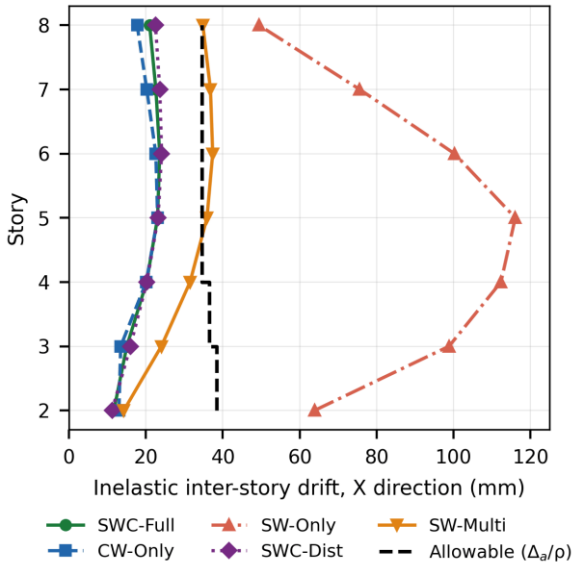


Figure 5. Comparison of Inter-Story Drift in the X Direction

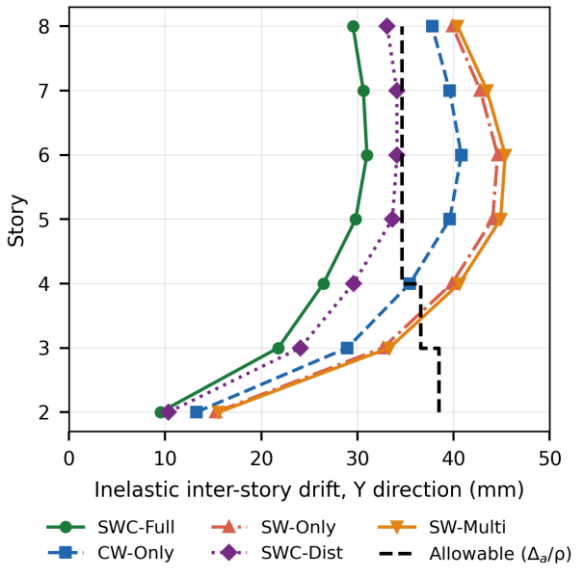


Figure 6. Comparison of Inter-Story Drift in the Y Direction

For the P-Delta analysis, all configurations formally satisfy the stability requirement $\theta < \theta_{allow} = 0.0909$ at every story, as shown in Table 4, but the margins differ by more than an order of magnitude. Four configurations remain below $\theta = 0.010$, whereas SW-Only reaches $\theta = 0.089$ at story 3 in the X direction, only 2% below the allowable limit. This peak occurs in the X direction, the same direction in which SW-Only exhibits its largest inter-story drift (116.03 mm at story 5 against an allowable 34.62 mm), which confirms that removing the core wall

severely reduces the lateral stiffness of the structure in that direction.

Table 4. Maximum P-Delta Stability Coefficient (θ_{max}) of Each Configuration

Configuration	θ_{max} (X)	θ_{max} (Y)	θ_{allow}	Status
SWC-Full	0.007	0.009	0.0909	OK
CW-Only	0.002	0.004	0.0909	OK
SW-Only	0.089	0.005	0.0909	OK
SWC-Dist	0.002	0.003	0.0909	OK
SW-Multi	0.004	0.005	0.0909	OK

The FEMA 440 P-Delta modification factor C_3 equals 1.000 for all configurations in both directions, indicating that second-order effects do not amplify the target displacement, because the pushover curves retain a positive post-yield stiffness, except for a local drop in base shear of SWC-Full in the Y direction that is discussed with Table 12. For the four configurations with $\theta < 0.010$ this is also consistent with the elastic stability check. For SW-Only, however, $C_3 = 1.000$ should not be read as a large reserve of stability: its elastic stability coefficient is already at the allowable limit, so any further reduction in lower-story stiffness would make the configuration unacceptable.

Dual System Effectiveness

Table 5 presents the seismic force distribution between the frame and the shear walls, which is also illustrated in Figure 7. The dual system was checked against SNI 1726:2019 Pasal 7.2.5.1 [2], which requires the moment frames to resist at least 25% of the design seismic force and the total seismic force to be resisted by the frames and walls in proportion to their rigidities. All configurations satisfy this requirement in both directions, but the distribution of the force differs significantly.

Table 5. Seismic Force Distribution in the Dual System

Config.	SW (X)	Frame (X)	SW (Y)	Frame (Y)	Remarks
SWC-Full	53	47	61	39	Effective
CW-Only	34	66	75	25	Less effective
SW-Only	13	87	74	26	Ineffective
SWC-Dist	72	28	67	33	Effective
SW-Multi	64	36	67	33	Effective

Note: SW = shear wall; values are percentages of the total base shear. All configurations meet SNI 1726:2019 Pasal 7.2.5.1 (frame ≥ 25%); the Remarks column describes the proportionality of the force share, which is not a code criterion.

SWC-Full shows the most balanced distribution (47% frame and 53% shear wall in the X direction). The 50:50 distribution used as a comparative benchmark in the scoring system reflects the proportional cooperation between the lateral elements and is not a code requirement; SNI 1726:2019 mandates only a minimum frame contribution of 25%. The shares were obtained from the base joint reactions of the scaled response spectrum cases (Spec X for FX and Spec Y for FY). The reactions of all base joints were summed to give the total base shear, the reactions of the base joints that belong to the shear walls and core wall were summed to give the wall share, and the frame share is the difference between the two. Because each joint reaction is a modal peak value, the sum of the joint reactions (12,303 kN in the X direction for SWC-Full) is about 10% larger than the modal base shear (11,129 kN), so the shares are approximate but consistent between the configurations. In contrast, SW-Only shows an extreme imbalance (87% frame in the X direction), indicating that the dual system is effectively non-functional in that direction because the shear walls absorb only 13% of the seismic force. This confirms that dual system effectiveness depends strongly on the proportional contribution of each element, as also reported by Katrangi et al. [8].

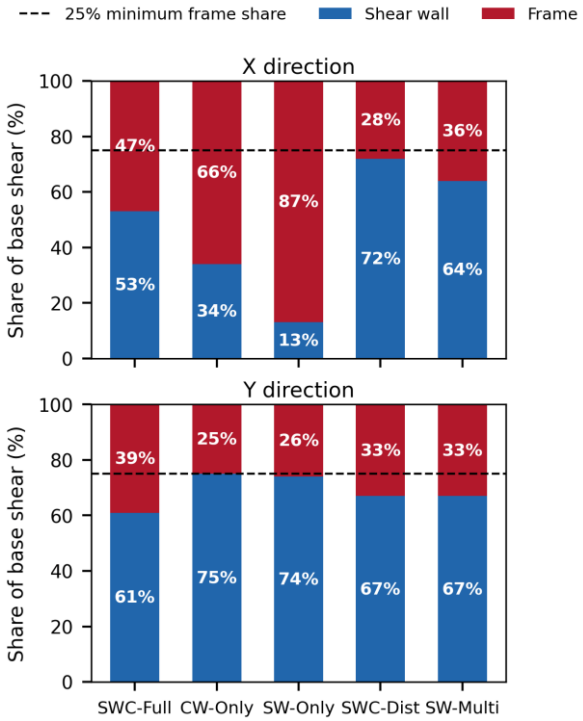


Figure 7. Seismic Force Distribution Between Shear Walls and Frame in the Dual System

Structural Element Compliance with SMRF Requirements

Table 6 summarizes the compliance evaluation of structural elements against the SMRF requirements of SNI 2847:2019 for the largest beam (350 × 650 mm) and column (700 × 700 mm).

The element forces were taken from the envelope of the SNI 1726:2019 load combinations [2], namely the basic combinations and the seismic combinations of Pasal 4.2.2.3, $(1.2 + 0.2S_{DS})D + \rho Q_E + L$ and $(0.9 - 0.2S_{DS})D + \rho Q_E$, with the redundancy factor $\rho = 1.3$ and the orthogonal effects combined by the 100%–30% rule (16 seismic combinations). The beam checked is the most heavily loaded B1 beam (350 × 650 mm, span 8.0 m, clear span 7.3 m, effective depth 590.5 mm). Flexure was checked at the support face for the negative and positive moments and at midspan. Shear was checked at the support, within the 2h = 1,300 mm plastic hinge region, with the capacity design shear $V_e = V_g + (M_{pr}^+ + M_{pr}^-)/\ell_n$, where the probable moments M_{pr} are based on $1.25f_y$, and at midspan with the shear from the analysis; because the factored torsion exceeded the threshold torsion ϕT_{th} in all configurations, torsion reinforcement was designed and the longitudinal reinforcement for combined flexure and torsion ($A_s + A_\ell$) was checked; T_{th}. The column checked is the 700 × 700 mm K1 column of the lowest story with D25 longitudinal bars and D10 ties; six force sets taken from the envelope (maximum and minimum P, M_2 and M_3) were checked with SP-Column, and the governing ratio occurred at P_u = 3,251.7 kN. Strength reduction factors of 0.90 for tension-controlled flexure and 0.75 for shear were used, following SNI 2847:2019 [17].

Table 6. Compliance Matrix of Structural Elements Against SMRF Requirements

Element / Parameter	SWC-Full	CW-Only	SW-Only	SWC-Dist	SW-Multi
Beam – flexure ($\phi M_n > M_u$)	OK	OK	Failed	OK	OK
Beam – shear ($\phi V_n/V_u \geq 1$)	OK	OK	OK	OK	OK
Beam – flexure + torsion ($A_s + A_\ell$)	OK	OK	Failed	OK	OK
Column – P-M diagram (SP-Column)	OK	OK	OK	OK	OK
Column – SCWB ($\Sigma M_{nc} \geq 1.2\ \Sigma M_{nb}$)	OK	OK	OK	OK	OK
Shear wall – shear capacity	OK	Failed	OK	OK	OK
Beam–column joint	Add. reinf.	Add. reinf.	Add. reinf.	Add. reinf.	Add. reinf.

Note: $T_u > \phi T_{th}$ in all configurations, so torsion reinforcement is required; the torsion row checks $A_s + A_\ell$ provided against required. T_{th} is the threshold torsional moment ($T_{th} = T_{cr}/4$). "Add. reinf." indicates that additional transverse reinforcement (four D10 legs at 150 mm spacing) is required at the beam–column joint.

SW-Only fails the beam flexural and torsional checks because the factored negative moment at the support (M_u = 933.40 kN·m) exceeds the design flexural strength (ϕM_n = 656.48 kN·m) by 42%, owing to internal force redistribution after the removal of the core wall; for the same reason the longitudinal reinforcement required for combined flexure and torsion at the support (83.61 cm^2) exceeds that provided (67.69 cm^2). This redistribution is consistent with the concept that the loss of a central stiffness element forces the remaining members to carry a larger proportion of the load [7]. CW-Only fails the shear capacity check of the shear wall because the design shear demand on the remaining wall (V_u/ϕ = 13,763 kN) is about twice that of SWC-Full (6,697 kN). All configurations require additional transverse reinforcement at the beam–column joints (four D10 legs at 150 mm spacing).

The beam–column joint shear check gives V_u = 3,384.0 kN against a design shear strength $\phi V_n = \phi(1.7\sqrt{f'_c})A_j = 0.8 \times 1.7 \times \sqrt{30} \times 490{,}000 = 3{,}650.0$ kN, where ϕ = 0.80 was used, which is conservative relative to ϕ = 0.85 for joints in SNI 2847:2019 Pasal 21.2.4.3, and $A_j = 700 \times 700\ mm^2$ is the effective joint area. The resulting demand-to-capacity ratio of 0.93 confirms joint shear adequacy for all configurations. The SCWB evaluation was carried out at the maximum axial load (P_u = 3,251.7 kN), which corresponds to the critical lower-story column.

Tables 7 and 8 present the detailed calculation results based on the ETABS output. Table 7 compares M_u against ϕM_n and the shear demand against ϕV_n for the beam, while Table 8 shows the capacity ratios obtained from the column check using SP-Column for each configuration.

Table 7. Beam Flexural and Shear Capacity Check for Each Configuration

Parameter	SWC-Full	CW-Only	SW-Only	SWC-Dist	SW-Multi	Unit
Flexure – negative support and positive span						
ϕM_n	656.48	656.48	656.48	656.48	656.48	kN·m
M_u	518.03	370.70	933.40	331.92	467.73	kN·m
Check $\phi M_n > M_u$	OK	OK	Failed	OK	OK	–
Flexure – positive support and negative span						
ϕM_n	561.36	561.36	561.36	561.36	561.36	kN·m
M_u	121.91	196.47	719.29	160.50	342.84	kN·m
Check $\phi M_n > M_u$	OK	OK	Failed	OK	OK	–
Support shear design						
V_n	939.57	747.12	747.12	747.12	747.12	kN
V_u	502.31	375.46	384.05	374.10	318.29	kN
$\phi V_n / V_u$	1.40	1.49	1.46	1.50	1.76	–
Capacity check	OK	OK	OK	OK	OK	–
Span shear reinforcement						
V_n	815.76	815.76	815.76	815.76	815.76	kN
$\phi V_n / V_u$	2.13	4.04	1.69	4.10	2.13	–
Capacity check	OK	OK	OK	OK	OK	–

Table 8. Column Capacity Check (SP-Column) and Strong Column–Weak Beam Evaluation

Parameter	SWC-Full	CW-Only	SW-Only	SWC-Dist	SW-Multi
Capacity ratio (SP-Column)	0.87	0.73	0.99	0.53	0.84
M_{nc} (kN·m)	1411.2	1448.6	1448.6	1448.6	1448.6
M_n^- (kN·m)	729.4	729.4	729.4	729.4	729.4
M_n^+ (kN·m)	623.7	623.7	623.7	623.7	623.7

Pushover Performance

Tables 9 and 10 present the displacement modification coefficients of Equation (1) used to compute the target displacement of each configuration in the X and Y directions, respectively. The coefficients comprise the modal participation factor (C_0), the inelastic modification factor (C_1), the hysteresis shape factor (C_2) and the P-Delta factor (C_3), together with the corresponding spectral acceleration (S_a), effective period (T_e), secant period at the performance point (T_{sec}) and resulting target displacement (δ_T). Because $T_e \geq T_s$ in all cases and the system is treated as non-degrading, $C_1 = C_2 = 1.0$ throughout, so the target displacements differ between configurations only through C_0, S_a and T_e.

Table 9. Target Displacement Coefficients (Equation (1)) in the X Direction

Coeff.	SWC-Full	CW-Only	SW-Only	SWC-Dist	SW-Multi
C_0	1.200	1.200	1.200	1.200	1.200
C_1	1.000	1.000	1.000	1.000	1.000
C_2	1.000	1.000	1.000	1.000	1.000
C_3	1.000	1.000	1.000	1.000	1.000
S_a (g)	1.267	1.081	0.453	1.577	1.187
T_e (s)	0.829	0.823	2.181	0.874	1.063
T_{sec} (s)	0.631	0.680	1.662	0.602	0.754
δ_T (mm)	259.80	218.55	643.16	359.59	400.41

Table 10. Target Displacement Coefficients (Equation (1)) in the Y Direction

Coeff.	SWC-Full	CW-Only	SW-Only	SWC-Dist	SW-Multi
C_0	1.200	1.200	1.200	1.200	1.200
C_1	1.000	1.000	1.000	1.000	1.000
C_2	1.000	1.000	1.000	1.000	1.000
C_3	1.000	1.000	1.000	1.000	1.000
S_a (g)	1.270	0.967	1.085	1.118	1.080
T_e (s)	0.959	1.096	1.188	0.938	1.215
T_{sec} (s)	0.683	0.830	0.832	0.715	0.845
δ_T (mm)	349.68	346.72	457.12	293.73	475.90

Note: $C_3 = 1.000$ in all cases, indicating that second-order effects do not amplify the target displacement. $C_1 = 1.0$ because $T_e \geq T_s = 0.806$ s and $C_2 = 1.0$ for non-degrading systems in all cases (FEMA 356 Section 3.3.3.3.2). $C_0 = 1.2$ for all configurations (FEMA 356 Table 3-2). T_{sec} is the secant period at the performance point ($S_d = S_a \cdot T_{sec}^2 / 4\pi^2 \cdot g$).

Table 11 presents, for each configuration and direction, the roof displacement at the FEMA 440 performance point, the target displacement δ_T, the roof drift ratio δ_T/H with H = 32.5 m, and the

resulting drift-based performance level, which are also illustrated in Figures 8 to 10. The thresholds are 325 mm (1%) for IO, 650 mm (2%) for LS and 1,300 mm (4%) for CP, as defined in the Method [21]. The target displacement exceeds the performance-point displacement in eight of the ten cases (by a factor of 1.26 to 1.63) and is used for the classification; in SWC-Full X and CW-Only X the performance-point displacement is the larger value (268.19 mm and 284.40 mm), but it is still below the IO threshold, so the classification does not change.

Table 11. Summary of Performance-Point Displacements, Target Displacements, Roof Drift Ratios and Drift-Based Performance Levels

Parameter	SWC-Full	CW-Only	SW-Only	SWC-Dist	SW-Multi
Target δ, X (mm)	259.80	218.55	643.16	359.59	400.41
S_a, X (g)	1.267	1.081	0.453	1.577	1.187
T_e, X (s)	0.829	0.823	2.181	0.874	1.063
PP roof displacement, X (mm)	268.19	284.40	417.35	286.31	303.16
δ_T/H, X (%)	0.80	0.67	1.98	1.11	1.23
Drift-based level X	IO	IO	LS	LS	LS
Target δ, Y (mm)	349.68	346.72	457.12	293.73	475.90
S_a, Y (g)	1.270	0.967	1.085	1.118	1.080
T_e, Y (s)	0.959	1.096	1.188	0.938	1.215
PP roof displacement, Y (mm)	230.14	259.85	284.37	221.37	291.35
δ_T/H, Y (%)	1.08	1.07	1.41	0.90	1.46
Drift-based level Y	LS	LS	LS	IO	LS

Note: δ = displacement; S_a = spectral acceleration; T_e = effective period; PP = FEMA 440 performance point; H = 32.5 m; levels follow the FEMA 356 Table C1-3 drift values for concrete frames (IO ≤ 1%, LS ≤ 2%, CP ≤ 4%).

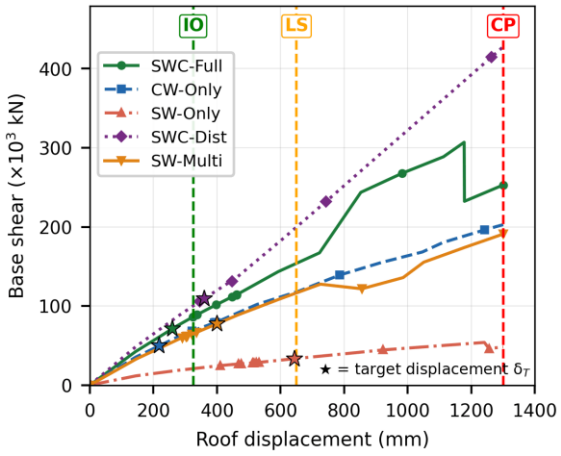


Figure 8. Pushover Capacity Curve in the X Direction

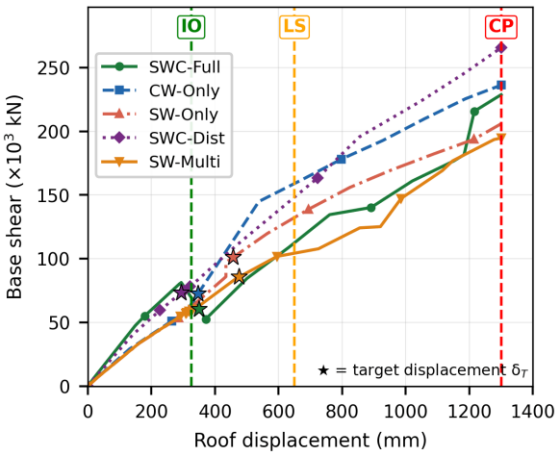


Figure 9. Pushover Capacity Curve in the Y Direction

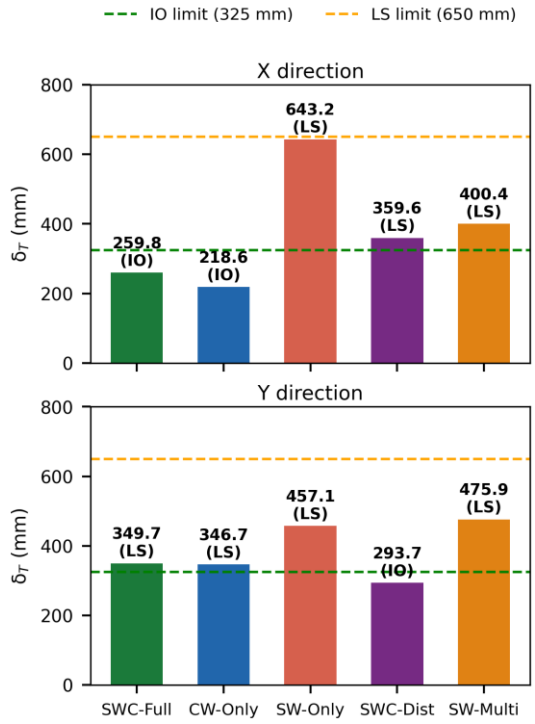


Figure 10. Target Displacement and Drift-Based Performance Level of Each Configuration

As shown in Figures 8, 9 and 10, a complementary pattern is observed between SWC-Full and SWC-Dist. SWC-Full reaches IO in the X direction (259.80 mm < 325 mm) but only LS in the Y direction, whereas SWC-Dist reaches IO in the Y direction (293.73 mm < 325 mm) but only LS in the X direction. This pattern indicates that the dominant orientation of the shear wall governs the stiffness distribution between the two principal directions and is consistent with Dumalanta et al. [9], who reported that specific shear wall configurations achieved the IO performance level in particular directions. SW-Only shows the poorest performance,

with an X-direction target displacement of 643.16 mm, only 1.1% below the LS limit of 650 mm, which represents a very small margin of safety in that direction.

The complementary performance pattern between SWC-Full and SWC-Dist reflects the directional stiffness distribution of their respective lateral element orientations. In SWC-Full the centrally placed core wall has its longer dimension aligned with the X direction, producing higher flexural stiffness and a smaller target displacement in X (259.80 mm → IO) while contributing less stiffness in Y (349.68 mm → LS). In SWC-Dist the redistributed shear wall positions increase the lever arm of the lateral elements relative to the center of mass in the Y direction, improving the Y-direction stiffness (293.73 mm → IO) at the cost of reduced X-direction performance (359.59 mm → LS). This trade-off illustrates a general characteristic of irregular structures: stiffness optimization in one principal direction typically reduces performance in the orthogonal direction, a limitation that can only be overcome through a symmetric shear wall distribution or three-dimensional optimization.

Component Acceptance at the Target Displacement

The drift-based level in Table 11 is a global indicator and not a component acceptance check. Table 12 therefore reports the state of the beam and column hinges, relative to the ASCE 41-17 acceptance criteria assigned in ETABS [20], at the analysis step closest to δ_T. In the three cases with a drift-based IO level (SWC-Full X, CW-Only X and SWC-Dist Y), 97.5–99.8% of the hinges remain within the IO criterion, but 6 to 82 hinges have passed it, and in SWC-Full X and CW-Only X one hinge has also passed the LS criterion. In the LS cases the number of hinges beyond IO ranges from 48 to 394. The most severe case is SWC-Full in the Y direction: the step closest to δ_T (370.7 mm) follows a local drop in base shear between 294 mm and 371 mm, and 23 hinges exceed the CP criterion at that step. If every primary component is required to satisfy its acceptance criterion, as in ASCE 41-17, the drift-based levels are therefore optimistic, most markedly for SWC-Full in the Y direction, which requires confirmation with a nonlinear wall model. Because the analysis steps are discrete, the step closest to δ_T may lie up to 65 mm away from δ_T (SW-Multi X).

Table 12. Hinge States at the Analysis Step Closest to the Target Displacement

Parameter	SWC-Full	CW-Only	SW-Only	SWC-Dist	SW-Multi
Step roof displacement, X (mm)	275.4	275.4	661.7	345.4	465.2
Hinges within A–IO, X (%)	99.8	99.8	87.9	98.5	96.1
IO–LS / LS–CP / >CP, X	5 / 1 / 0	6 / 1 / 0	318 / 74 / 2	47 / 1 / 0	125 / 0 / 1
Step roof displacement, Y (mm)	370.7	306.5	434.2	297.7	465.2
Hinges within A–IO, Y (%)	88.3	97.8	98.0	97.5	96.6
IO–LS / LS–CP / >CP, Y	273 / 81 / 23	73 / 0 / 0	63 / 1 / 0	82 / 0 / 0	100 / 12 / 0
Total number of hinges	3222	3250	3264	3218	3250

Note: hinge states from the ETABS pushover output; A–IO = within the IO criterion; IO–LS, LS–CP and >CP = number of hinges beyond the IO, LS and CP criteria.

Comprehensive Evaluation

To provide a quantitative comparison across configurations, a relative performance score (S) was computed for the seven parameters using capacity-to-demand ratio normalization. Each parameter was normalized to the range 0–1, where 1 indicates the best performance and 0 indicates failure. The normalization rules are as follows.

(1) Inter-story drift: $S = \min(\Delta_{allow}/\Delta_{max}, 1.0)$, with a 50% penalty for failure in one direction and a zero score for failure in both directions.

(2) P-Delta stability: $S = 1 - (\theta_{max} / \theta_{allow})$, where $\theta_{allow} = 0.0909$.

(3) Dual system effectiveness: $S = 1 - |\%frame - 50| / 50$, measuring the deviation from a 50:50 distribution between frame and shear wall. The worst value of the X and Y directions is used.

(4) SMRF beam: $S = \min(\phi M_n/M_u, \phi V_n/V_u, \phi T_n/T_u)$, capped at 1.0; the governing value of the flexural, shear and torsional checks is used.

(5) SMRF column: $S = \min(\Sigma M_{nc} / (1.2\ \Sigma M_{nb}), 1.0)$, based on the strong column–weak beam criterion.

(6) Shear wall capacity: S = 1.0 if all shear wall checks are satisfied and 0 otherwise.

(7) Pushover performance level: IO = 1.00, LS = 0.50, CP = 0.00 per direction; the final score is the average of both directions.

The scoring system is a comparative evaluation framework developed in this study to provide a quantitative ranking across configurations; it is not a standardized procedure. The dual system score uses the deviation from a 50:50 distribution as a proportionality indicator, acknowledging that SNI 1726:2019 requires only a frame contribution of at least 25%. Its sensitivity to

these scoring choices is examined after Table 14; a formal weighting study is recommended for future research.

Table 13 presents the compliance-based evaluation scorecard, while Table 14 gives the quantitative normalized scores, which are visualized in Figure 11.

Table 13. Compliance Evaluation Scorecard of All Configurations

Parameter	SWC-Full	CW-Only	SW-Only	SWC-Dist	SW-Multi
Drift X and Y	✓	✗	✗	✓	✗
P-Delta	✓	✓	✓	✓	✓
Dual system	✓	△	✓	✓	✓
SMRF beam	✓	✓	✗	✓	✓
SMRF column	✓	✓	✓	✓	✓
Shear wall	✓	✗	✓	✓	✓
Pushover X	IO	IO	LS	LS	LS
Pushover Y	LS	LS	LS	IO	LS
Total failures	0	2	2	0	1

Note: ✓ = compliant; ✗ = non-compliant; △ = at the limit. Dual system = SNI 1726:2019 Pasal 7.2.5.1 (frame share ≥ 25%); the proportionality of the force share is scored separately in Table 14.

Table 14. Relative Performance Scores Based on Capacity-to-Demand Ratio Normalization

Parameter	SWC-Full	CW-Only	SW-Only	SWC-Dist	SW-Multi
Inter-story drift	1.00	0.42	0.00	1.00	0.00
P-Delta stability	0.90	0.96	0.02	0.97	0.95
Dual system effectiveness	0.78	0.50	0.26	0.56	0.66
SMRF beam	1.00	1.00	0.70	1.00	1.00
SMRF column	1.00	1.00	1.00	1.00	1.00
Shear wall capacity	1.00	0.00	1.00	1.00	1.00
Pushover performance level	0.75	0.75	0.50	0.75	0.50
Average	0.92	0.66	0.50	0.90	0.73

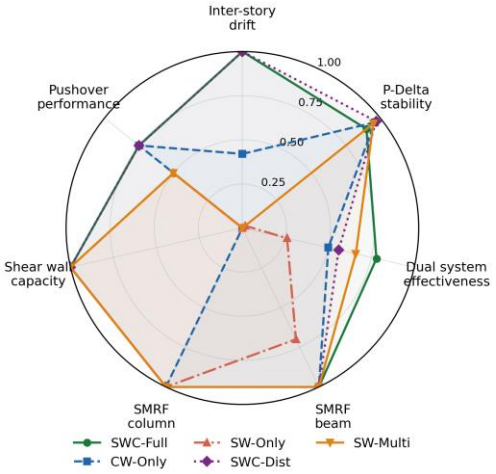


Figure 11. Relative Performance Radar Chart of the Five Shear Wall Configurations

Based on the average scores, SWC-Full (0.92) and SWC-Dist (0.90) rank highest, confirming that the complete combination of shear wall and core wall is the determining factor in satisfying all seismic requirements. Both configurations achieve a perfect score (1.00) in four of the seven parameters. SW-Only has the lowest score (0.50), with critical weaknesses in inter-story drift (0.00), P-Delta margin (0.02), dual system effectiveness (0.26) and beam capacity (0.70), demonstrating the cascading effect of removing the core wall on both the global response and the element-level behavior. CW-Only (0.66) and SW-Multi (0.73) rank in the middle, each with one critical weakness: CW-Only in shear wall capacity (0.00) and SW-Multi in drift (0.00). The contrast between Table 13 and Table 14 for the P-Delta row illustrates the purpose of the two tables: Table 13 records code compliance, which SW-Only formally achieves, whereas Table 14 measures the remaining margin, which for SW-Only is almost exhausted.

The difference of 0.02 between SWC-Full and SWC-Dist is too small to rank one above the other with confidence. Two simple checks show this. First, if the dual system parameter is scored only against the code requirement of SNI 1726:2019 Pasal 7.2.5.1 (score 1.0 when the frame share is at least 25%) instead of the deviation from 50:50, the averages become 0.95 for SWC-Full and 0.96 for SWC-Dist, which reverses the order. Second, if each of the seven parameters is removed in turn, the difference between the two ranges from −0.01 to +0.04. In every variant, however, both configurations remain ahead of the other three by at least 0.03. SWC-Full and SWC-Dist are therefore regarded as equivalent within the resolution of the scoring framework, and the choice between them should be based on the direction in which the higher performance level is required.

Discussion

The results indicate that the seismic response of the GLU building is governed less by the amount of shear wall than by the position of the walls relative to the center of rigidity. The torsional stiffness provided by a wall increases with the square of its distance from the center of rigidity, so the centrally placed core wall of SWC-Full and CW-Only adds considerable translational stiffness but comparatively little torsional stiffness. This explains why both configurations exhibit a rotational first mode, with torsional mass participation ratios of

0.242 and 0.266, and why the existing building (SWC-Full) shows $\Delta_{max}/\Delta_{avg}$ ratios of up to 1.488 in the X direction and 1.597 in the Y direction. Moving part of the walls away from the plan center, as in SWC-Dist, lengthens the torsional lever arm; the first mode then becomes translational and the fundamental period becomes the shortest of all configurations (0.876 s). The irregularity class, however, does not change: SWC-Dist has the largest ratio of all configurations (1.681 in the Y direction, Table 3), and its upper-story ratios in the X direction (1.31–1.35) equal those of SWC-Full. SW-Multi replaces the core with open walls oriented in the X direction, yet its period is longer (1.025 s) and it fails the drift limit in both directions, which shows that open linear walls cannot reproduce the combined flexural and torsional stiffness of a closed core.

These trends agree with previous parametric studies. Kurnia et al. [12] found that the most effective shear wall position in an irregular building reduced the maximum lateral displacement by about 40% in the X direction (from 157.57 mm to 94.46 mm) and 38% in the Y direction (from 193.13 mm to 119.24 mm) relative to the building without shear walls. In the present study the contrast between the stiffest (SWC-Dist) and the most flexible (SW-Only) configuration is even larger: the fundamental period almost doubles, from 0.876 s to 1.673 s, and the maximum X-direction drift increases almost fivefold, from 24.10 mm to 116.03 mm. Pranava et al. [5] and Khelaifia et al. [10] likewise reported that optimized and complete wall layouts minimize torsional irregularity and drift, and Dumalanta et al. [9] observed an improvement from LS to IO when the walls were distributed. The present study extends these observations to a Risk Category IV dual system and shows that the same configuration change also governs the force share between walls and frames and the SMRF compliance of the beams, which studies limited to global drift did not evaluate.

The element-level results reveal a cascading mechanism that drift checks alone do not show. When the core wall is removed (SW-Only), the walls carry only 13% of the X-direction base shear and the frames must resist the remaining 87%. The beam flexural failure (M_u = 933.40 kN·m, 42% above ϕM_n = 656.48 kN·m) and the beam torsional failure follow directly from this redistribution. A dual system can therefore satisfy the 25% minimum frame share of SNI 1726:2019 even when the walls are almost inactive, so the minimum frame share alone is not a sufficient indicator of dual system performance. This observation agrees with Katrangi et al. [8], who showed that the base shear contribution ratios depend on the relative stiffness of the walls and frames, and with Yakhkeshi and Tehrani [14], who found that wall geometry rather than wall area controls the collapse resistance. Conversely, CW-Only retains the core and satisfies the beam checks, but the shear demand concentrated on the remaining wall (V_u/ϕ = 13,763 kN, about twice that of SWC-Full) exceeds its capacity. Removing the perimeter walls therefore shifts the vulnerability from the frames to the walls rather than eliminating it.

The pushover results place all configurations between the IO and LS levels on the drift-based scale, although some hinges already exceed the IO criterion at δ_T (Table 12). Usman et al. [24], who applied the same coefficient method with the FEMA 440 performance point to a four-story reinforced concrete shear wall building in several Indonesian cities, including Bandar Lampung, obtained the IO level for most locations. The larger target displacements in the present study (218.55 mm to 643.16 mm) are consistent with the greater height of the GLU building (32.5 m compared with about 17 m) and its longer effective periods (0.823 s to 2.181 s compared with about 0.56 s). The complementary pattern of SWC-Full and SWC-Dist shows that a configuration that is optimal in one direction is not necessarily optimal in the other, so the selection must consider both principal directions. SW-Only formally attains the LS level, but its X-direction target displacement is only 1.1% below the LS limit and its stability coefficient (θ = 0.089) is close to the allowable value of 0.0909. This configuration therefore has practically no reserve against uncertainties in the ground motion, material properties or modeling assumptions.

From a design perspective, the findings suggest three practical guidelines for irregular Risk Category IV buildings: the core wall should be retained, because its removal produced the most severe failures (a 42% beam flexural overstress, the largest drift exceedance and the smallest wall share of the base shear); perimeter or distributed walls should be added to increase the torsional lever arm rather than only the total wall area; and dual system adequacy should be judged from the actual force share and the resulting element demands, not only from the 25% minimum frame share. SWC-Full and SWC-Dist both satisfy these guidelines, and the choice between them can be based on the direction in which the higher performance level (IO) is required, for example the direction that governs the

protection of critical occupancies or nonstructural components.

CONCLUSIONS

Based on the comprehensive analysis of five shear wall configurations in the ITERA Public Service Building, the shear wall configuration significantly affects the torsional response of the structure. Centralized placement (SWC-Full) produces a first rotational mode (RZ), whereas distributed placement (SWC-Dist) produces a translational mode (UX), and the X-direction period ranges from 0.876 s (SWC-Dist) to 1.673 s (SW-Only), demonstrating a substantial effect on the lateral stiffness of the structure. Only SWC-Full and SWC-Dist satisfy all seven evaluation criteria simultaneously (inter-story drift, P-Delta stability, dual system, SMRF beam and column compliance, shear wall capacity and pushover performance) without a single failed criterion; the critical commonality of both is the retention of the complete shear wall and core wall combination. Removal of the core wall (SW-Only) has the most detrimental effect, with failures in inter-story drift and beam capacity: the factored beam moment exceeds the design flexural strength by 42%, and although the 25% minimum frame share of SNI 1726:2019 Pasal 7.2.5.1 is met, the walls carry only 13% of the X-direction base shear, and the pushover target displacement approaches the Life Safety limit. SWC-Full and SWC-Dist exhibit a complementary performance pattern, in which SWC-Full attains IO in the X direction but LS in the Y direction while SWC-Dist attains the reverse, indicating that the dominant orientation of the shear wall governs the stiffness distribution and performance level between directions. Their relative scores (0.92 and 0.90) are equivalent within the sensitivity of the scoring framework, so both configurations are recommended for the structural design of the ITERA GLU.

The main limitations of this study are as follows. The shear walls were modeled as elastic shell elements, so wall yielding and degradation are not captured and the capacity curves overestimate the stiffness and strength of the system. This simplification does not change the main conclusion, because the objective of the study is to identify the most suitable shear wall configuration rather than to estimate the absolute nonlinear capacity of the building. The same modeling assumptions were applied to all five models, so the differences between the results reflect the wall layout. In addition, six of the seven evaluation parameters (drift, P-Delta stability, dual system, SMRF beam and column compliance and shear wall capacity) were obtained from the elastic analysis and the code-based element checks, which do not depend on the nonlinear behavior of the walls. The performance levels are based on the FEMA 356 drift values for concrete frames, which are indicative values rather than acceptance criteria, and the hinge states at the target displacement show that some components already exceed the IO criterion; the levels are therefore upper-bound, comparative estimates. Soil–structure interaction was not considered, and the scoring framework was checked only with simple variants. Future research is recommended to use nonlinear wall models (for example fiber or layered shell elements), to evaluate the performance levels with component-based acceptance criteria, and to include soil–structure interaction and a formal weighting study.

ACKNOWLEDGMENT

The authors gratefully acknowledge the financial support of Institut Teknologi Sumatera through the 2026 *Penelitian Berbasis Kepakaran* research grant (Contract No. 2269aq/DST/IT9.2.1/PT.01.03/2026). The authors also thank the project development team of the ITERA Public Service Building (GLU) for providing the data used in this study.

AUTHOR DECLARATION

Authors' Contributions and Responsibilities

All authors contributed to the study conception and design, participated in the data analysis and interpretation of the results, and contributed to the writing of the manuscript.

Funding

This work was supported by the *Penelitian Berbasis Kepakaran* research grant of the Institute for Research and Community Service (LPPM), Institut Teknologi Sumatera, in 2026.

Availability of Data and Materials

The data that support the findings of this study are available from the corresponding author upon reasonable request.

Competing Interests

The authors declare that they have no known competing financial interests or personal relationships that could have appeared to influence the work reported in this paper.

REFERENCES

[1] W. Triyoso, W. Kongko, G. S. Prasetya, and A. Suwondo, "Study on earthquake and tsunami hazard: evaluating probabilistic seismic hazard function (PSHF) and potential tsunami height simulation in the coastal cities of Sumatra Island," *Frontiers in Built Environment*, vol. 10, Art. no. 1310251, 2024, doi: 10.3389/fbuil.2024.1310251.

[2] Badan Standardisasi Nasional, *Tata Cara Perencanaan Ketahanan Gempa untuk Struktur Bangunan Gedung dan Nongedung (SNI 1726:2019)*. Jakarta, Indonesia: Badan Standardisasi Nasional, 2019.

[3] M. Aslani and P. Tehrani, "Seismic response and collapse capacity assessment of dual RC buildings with vertical irregularities in shear walls," *Scientific Reports*, vol. 15, Art. no. 9966, 2025, doi: 10.1038/s41598-025-94328-z.

[4] S. Ruggieri and V. Vukobratović, "The influence of torsion on acceleration demands in low-rise RC buildings," *Bulletin of Earthquake Engineering*, vol. 22, no. 5, pp. 2433–2468, 2024, doi: 10.1007/s10518-024-01873-5.

[5] K. Pranava, A. R. Avinash, M. Chaithra, S. Anil, and K. Kamath, "Seismic performance of torsionally irregular multistorey RC buildings with optimised shear wall configurations," *Infrastructures*, vol. 10, no. 11, Art. no. 296, 2025, doi: 10.3390/infrastructures10110296.

[6] P. V. Shamrao, "Seismic fragility analysis for torsionally imbalanced shear wall concrete building," *Journal of The Institution of Engineers (India): Series A*, vol. 102, no. 2, pp. 553–563, 2021, doi: 10.1007/s40030-021-00527-y.

[7] F. Velarde *et al.*, "Structural reliability assessment of dual RC buildings for different shear wall configuration," *Buildings*, vol. 15, no. 11, Art. no. 1783, 2025, doi: 10.3390/buildings15111783.

[8] M. Katrangi, M. M. Memarpour, and M. Yakhchalian, "Assessment of the seismic performance and the base shear contribution ratios of the RC wall-frame dual system considering soil–structure interaction," *Journal of Earthquake Engineering*, vol. 26, no. 10, pp. 5290–5317, 2022, doi: 10.1080/13632469.2021.1871678.

[9] M. C. R. Dumalanta, N. G. I. Rabilas, A. J. C. Rapacon, E. J. S. Urieta, and G. A. Frando, "Seismic performance evaluation of an irregular five-story reinforced concrete building under various shear wall placement configurations using pushover analysis," *The Vector: International Journal of Emerging Science, Technology and Management (IJESTM)*, vol. 34, no. 1, 2025. [Online]. Available: https://vector.unp.edu.ph/index.php/1/article/view/340. [Accessed: Oct. 9, 2026].

[10] A. Khelaifia, R. Chebili, and A. Zine, "Impact of the position and quantity of shear walls in buildings on the seismic performance," *Asian Journal of Civil Engineering*, vol. 25, no. 1, pp. 953–964, 2024, doi: 10.1007/s42107-023-00824-w.

[11] M. Barser, R. C. Bush, and A. I. Shirkol, "Performance analysis of asymmetrical RC structures using different configurations of shear wall," *Materials Today: Proceedings*, vol. 88, pp. 52–65, 2023, doi: 10.1016/j.matpr.2023.04.493.

[12] A. Kurnia, S. H. Dewi, and M. Kurniawan, "Pengaruh posisi dinding geser terhadap kinerja struktur pada gedung tidak beraturan dengan menggunakan metode response spectrum [Effect of shear wall position on structural performance in irregular buildings using the response spectrum method]," *Jurnal Saintis*, vol. 18, no. 1, pp. 15–24, 2018, doi: 10.25299/saintis.2018.vol18(1).2809.

[13] M. A. Salmassi, A. Kheyroddin, and A. Hemmati, "Seismic behavior of end walls in RC tall buildings with torsional irregularity," *Magazine of Civil Engineering*, vol. 97, no. 5, Art. no. 9707, 2020, doi: 10.18720/mce.97.7.

[14] M. Yakhkeshi and P. Tehrani, "Seismic performance of dual RC frame-shear wall buildings with nonparallel shear walls: insights and recommendations," *Bulletin of Earthquake Engineering*, vol. 23, no. 11, pp. 4831–4869, 2025, doi: 10.1007/s10518-025-02233-7.

[15] RSA Cipta Karya, "Desain Spektra Indonesia 2021: aplikasi online spektrum respons," 2021. [Online]. Available: http://rsa.ciptakarya.pu.go.id/2021/. [Accessed: May 12, 2025].

[16] Badan Standardisasi Nasional, *Beban Desain Minimum dan Kriteria Terkait untuk Bangunan Gedung dan Struktur Lain (SNI 1727:2020)*.

Jakarta, Indonesia: Badan Standardisasi Nasional, 2020.

[17] Badan Standardisasi Nasional, *Persyaratan Beton Struktural untuk Bangunan Gedung (SNI 2847:2019)*. Jakarta, Indonesia: Badan Standardisasi Nasional, 2019.

[18] R. A. Firdha, M. Isneini, H. R. Husni, and R. Widyawati, "Structural performance analysis of multi-story buildings under seismic loads using pushover analysis method (case study: non-surgical inpatient building RSUD Dr. H. Abdul Moeloek)," *Jurnal Rekayasa Sipil dan Desain*, vol. 9, no. 4, pp. 829–840, 2021, doi: 10.23960/jrsdd.v9i4.2201.

[19] K. K. Kuria and O. K. Kegyes-Brassai, "Pushover analysis in seismic engineering: a detailed chronology and review of techniques for structural assessment," *Applied Sciences*, vol. 14, no. 1, Art. no. 151, 2024, doi: 10.3390/app14010151.

[20] American Society of Civil Engineers, *Seismic Evaluation and Retrofit of Existing Buildings (ASCE/SEI 41-17)*. Reston, VA, USA: ASCE, 2017, doi: 10.1061/9780784414859.

[21] Federal Emergency Management Agency, *Prestandard and Commentary for the Seismic Rehabilitation of Buildings (FEMA 356)*. Washington, DC, USA: FEMA, 2000.

[22] Federal Emergency Management Agency, *Improvement of Nonlinear Static Seismic Analysis Procedures (FEMA 440)*. Washington, DC, USA: FEMA, 2005.

[23] J. R. Sugianto and Y. A. Pranata, "Seismic performance evaluation using pushover analysis of four two-storey residential building types in West Bandung Regency," *Journal of Green Science and Technology*, vol. 10, no. 1, 2026, doi: 10.33603/jgst.v10i1.11748.

[24] A. P. Usman, Rosidawani, and S. P. Mutmainna, "Analisis respons dan kinerja struktur bangunan gedung menggunakan pushover analysis [Analysis of response and performance of building structures using pushover analysis]," *Jurnal Saintis*, vol. 21, no. 2, pp. 87–96, 2021, doi: 10.25299/saintis.2021.vol21(02).7585.

NOMENCLATURE

A_x	torsional amplification factor
C_0	factor relating spectral displacement to roof displacement
C_1	factor relating maximum inelastic to elastic displacement
C_2	factor for pinched hysteresis, stiffness degradation and strength deterioration
C_3	P-Delta factor
g	acceleration of gravity (9.81 m/s^2)
H	height of the monitored roof node above the base (32.5 m)
M_n^-, M_n^+	negative and positive nominal flexural strengths of the beam (kN·m)
S_a	spectral acceleration at the performance point (g)
T_e	effective period (s)
T_s	characteristic period of the design response spectrum, S_{D1}/S_{DS} (s)
T_{sec}	secant period at the performance point (s)
Δ_{max}, Δ_{avg}	maximum and average story displacement
δ_T	target displacement (mm)
θ, θ_{allow}	P-Delta stability coefficient and its allowable limit
ΣM_{nb}	sum of nominal flexural strengths of beams framing into the joint (kN·m)
ΣM_{nc}	sum of nominal flexural strengths of columns above and below the joint (kN·m)
ϕ	strength reduction factor

This page is intentionally blank